Marine Pollution Bulletin 176 (2022) 113476

Contents lists available at ScienceDirect

Marine Pollution Bulletin

journal homepage: www.elsevier.com/locate/marpolbul

Establishing historical ^{90}Sr activity in seawater of the China seas from 1963 to 2018

Wuhui Lin [a,b,d,*], Minting Mo [a], Kefu Yu [a,b,*], Jinqiu Du [c], Hongtao Shen [d], Yinghui Wang [a,b], Xianwen He [e], Liangliang Feng [e]

[a] School of Marine Sciences, Guangxi University, Nanning 530004, China
[b] Guangxi Laboratory on the study of Coral Reefs in the South China Sea, Nanning 530004, China
[c] National Marine Environmental Monitoring Center, Dalian 116023, China
[d] Guangxi Key Laboratory of Nuclear Physics and Nuclear Technology, Guangxi Normal University, Guilin 541004, China
[e] Radiation-Environment Management and Monitoring Station of Guangxi Zhuang Autonomous Region, Nanning 530222, China

ARTICLE INFO

Keywords:
Effective half-life
Radionuclides
Fukushima Nuclear Accident
Boundary scavenging
Marine biological pump

ABSTRACT

Historical ^{90}Sr activity in seawater was established in the China seas from 1963 to 2018. Based on the exponential decrease in ^{90}Sr activity in seawater, the effective half-life (EHL) of ^{90}Sr was quantified to be 11.5 ± 1.6 a, 16.5 ± 2.4 a, 27.2 ± 6.2 a, and 26.7 ± 4.3 a in the Bohai Sea, Yellow Sea, East China Sea, and South China Sea, respectively. We found contrasting patterns in the EHL of ^{90}Sr and ^{137}Cs in the marginal seas and open oceans that were closely related to the subtly different pathways of ^{90}Sr and ^{137}Cs in marine environment. Additionally, we demonstrated that Fukushima-derived ^{90}Sr (<0.01 Bq/m^3) would be difficult to identify in the China seas. Our study not only provided the key parameter of the EHL in marine models for predicting the ^{90}Sr activity in the China seas in the post-Fukushima era but also enhanced our understanding of ^{90}Sr behavior and its fate in marine environments.

1. Introduction

Known to be of great concern, the artificial radionuclide of ^{90}Sr is important because of its high fission yield (5.77% in ^{235}U-thermal neutron fission), relatively long physical half-life (28.8 a), high concentration factor in bone/skeleton, and high radiotoxicity in biotas and humans (Shao et al., 2018b; Burger and Lichtscheidl, 2019). Comparing to another important artificial radionuclide of ^{137}Cs, ^{90}Sr is more likely to migrate from the soil to groundwater and river water due to its higher mobility in the terrestrial environment (Saniewski and Zalewska, 2016). A lower sediment-seawater distribution coefficient (Kd) was observed for ^{90}Sr (Kd = 1 L/kg −100 L/kg) relative to that of ^{137}Cs (Kd = 100 L/kg −1000 L/kg) (IAEA, 2004; Takata et al., 2014, 2016), thereby implying low ability of adsorption onto particle surface and high mobility of ^{90}Sr in marine environments. However, the analytical method for ^{90}Sr is very complicated, labor-intensive and time-consuming because of its pure β emission and high intensive interferences (e.g., Ca, Mg, Sr, etc.) in marine environment (Vajda and Kim, 2010; Shao et al., 2018b). Even though ^{90}Sr has a high mobility relative to ^{137}Cs in the environment, the amount of available data on ^{90}Sr and our understanding of its transfer in marine food web were significantly less than that of ^{137}Cs data (Povinec et al., 2012; Steinhauser, 2014; Pan et al., 2016).

An enormous quantity of artificial radionuclides was released into the North Pacific Ocean after the Fukushima Nuclear Accident (FNA) (Lin et al., 2015; Lin et al., 2016; Buesseler et al., 2017). Fukushima-derived ^{90}Sr was among those released into marine environment, resulting in elevated ^{90}Sr activity in seawater (Povinec et al., 2012; Casacuberta et al., 2013; Men et al., 2015; Yu et al., 2015; Castrillejo et al., 2016; Kenyon et al., 2020), marine sediment (Nagaoka et al., 2015; Shozugawa et al., 2015), and marine biotas (Fujimoto et al., 2015; Karube et al., 2016; Miki et al., 2017). Recently, the abnormally high ^{90}Sr activity (up to 10^7 Bq/m^3) was also reported in the Fukushima radioactive wastewater after the treatment of the Advanced Liquid Processing Systems for removing artificial radionuclides before discharging into the Pacific Ocean (Buesseler, 2020; Lin et al., 2021; TEPCO, 2021). Additionally, the excess radiation dose rate derived from the elevated ^{90}Sr activity may be induced on marine biotas and humans by seafood consumption (Johansen et al., 2015; Men et al., 2017). However, the field observations of ^{90}Sr in marine environments were far less than that of ^{137}Cs after the FNA (Povinec et al., 2012; Steinhauser,

* Corresponding authors at: Office 1111#, Zonghe Shiyan Building, Guangxi University, Nanning City, Guangxi Province, China.
E-mail addresses: linwuhui8@163.com (W. Lin), kefuyu@scsio.ac.cn (K. Yu).

https://doi.org/10.1016/j.marpolbul.2022.113476
Received 13 January 2022; Received in revised form 16 February 2022; Accepted 16 February 2022

2014).

The activity of ^{90}Sr is a direct parameter to describe the pollution status in the environment for assessing the impact of nuclear facilities, nuclear accidents, radioactive waste dumping, and nuclear weapons testing. Moreover, the effective half-life (EHL) of ^{90}Sr is a key parameter in physical-biogeochemical models for predicting the ^{90}Sr activity in the environment (Pröhl et al., 2006). Generally, the EHL is calculated based on the time series of ^{90}Sr activity after exponential fitting (Merz et al., 2016).

The long-term time series of ^{90}Sr monitoring had been constructed for atmospheric aerosol during 1957– 2018 (Igarashi et al., 2015; Kinase et al., 2020), precipitation during 1963– 1999 (Ikeuchi, 2006), river water in Japan during 1963– 1999 (Ikeuchi, 2006) and Rhone River in France during 2002– 2018 (Eyrolle et al., 2020), seawater during 1960– 2002 (Kasamatsu and Inatomi, 1998; Povinec et al., 2005; Cigna, 2006), soil during 1975– 2013 (Robison et al., 2003; Corcho-Alvarado et al., 2016), marine sediment during 1963– 1999 (Ikeuchi, 2003; Ikeuchi, 2006), food during 1959– 2013 (Pröhl et al., 2006; Corcho-Alvarado et al., 2016; Merz et al., 2016), and terrestrial and marine biotas during 1965– 2002 (Pröhl et al., 2006; Morita et al., 2010). Particularly, the EHL of ^{90}Sr in seawater had been calculated in the Baltic Sea (Saniewski and Zalewska, 2018), East Sea/Sea of Japan (Hirose and Povinec, 2019), and Pacific Ocean and Indian Ocean (Povinec et al., 2005).

The China seas, including the Bohai Sea, Yellow Sea, East China Sea, and South China Sea, intensively exchange seawater with the North Pacific Ocean (Zheng et al., 2006). The radionuclides of ^{137}Cs and $^{239+240}$Pu were transported from the North Pacific Ocean and were accumulated and stored in the China seas (Zhang et al., 2019; Wu et al., 2020a; Cao et al., 2021). In the context of the FNA, ^{134}Cs derived from the FNA in seawater was observed at few stations in the Yellow Sea, East China Sea, and South China Sea due to the hydrological exchange between the China seas and the North Pacific Ocean (Inoue et al., 2018a; Deng et al., 2020; Wang et al., 2022). Meanwhile, ^{90}Sr was also released into the North Pacific Ocean after the FNA (Povinec et al., 2012; Lin et al., 2016). However, there is very limited data on ^{90}Sr in seawater in the China seas. To our knowledge, the EHL of ^{90}Sr has not been comprehensively studied in the China seas, in contrast to the EHL of ^{137}Cs, which has been studied in the Yellow Sea (Zhang et al., 2019; Wu et al., 2020b), East China Sea (Wu, 2018; Zhang et al., 2019; Wu et al., 2020b), and South China Sea (Wu, 2018; Wu et al., 2020b). Additionally, the impact of the FNA on the China seas has not been well discussed in the context of the long-term time series of ^{90}Sr activity in seawater, even though limited ^{90}Sr data in the South China Sea and East China Sea have been reported during 2011– 2014 after the FNA (Men et al., 2015; Zhou et al., 2018; Deng et al., 2020; Zhang et al., 2021).

In this study, the ^{90}Sr characteristics in the China seas were investigated from the perspectives of the ^{90}Sr activity and its EHL. The long-term time series of ^{90}Sr activity in seawater during 1963– 2018 were simultaneously established for the first time in the Bohai Sea, Yellow Sea, East China Sea, and South China Sea after compiling our measured ^{90}Sr data and data from many previous studies. The possible signal of the Fukushima-derived ^{90}Sr in the China seas was discussed on the basis of theoretical calculations and field observations. Our study will facilitate international communication on the historical ^{90}Sr activity in the China seas and provide a valuable supplement to the International Atomic Energy Agency's (IAEA) Marine Radioactivity Information System (MARIS) for identifying and assessing additional source terms of ^{90}Sr from nuclear accidents, nuclear reprocessing plants, radioactive waste dumping sites, and nuclear weapons testing sites in the North Pacific Ocean.

2. Materials and methods

2.1. Study areas

The China seas are located in the transitional region between the largest continent, Asian, and the largest ocean, the Pacific Ocean, with a typically broad continental shelf. The China seas have a total area of 4.73×10^6 km^2, with a total continental coastline of 1.8×10^4 km (Song, 2010). The China seas consist of the Bohai Sea, Yellow Sea, East China Sea, and South China Sea, extending from temperate to subtropical and tropical zones. The areas of the Bohai Sea, Yellow Sea, East China Sea, and South China Sea are 7.7×10^4 km^2, 3.8×10^5 km^2, 7.7×10^5 km^2, 3.5×10^6 km^2, with an average depth of 18.7 m, 44 m, 370 m, and 1212 m, respectively (Song, 2010). The three largest rivers in China discharging into the China seas are the Yellow River, Changjiang River, and Pearl River (Fig. 1), resulting in the accumulation of large amounts of nutrients and contaminants (e.g., heavy metals, organic pollutants, radionuclides, microplastics, etc.) in the China seas (Pan and Wang, 2012). The annual water discharges and sediment fluxes of the Yellow River, Changjiang River, and Pearl River are 4.2×10^{10} m^3/y and 1.0×10^9 t/y, 9.24×10^{11} m^3/y and 4.86×10^8 t/y, and 3.3×10^{11} m^3/y and 8.0×10^7 t, respectively (Song, 2010). Notice that the Changjiang River ranks third in length, fifth in fresh water discharge, and fourth in sediment discharge in the world (Song, 2010). What's more, the East China Sea has a close interaction with its surrounding environment of Kuroshio Current, Yellow Sea, and South China Sea. The East China Sea is a relatively open system and is more complicated than other China seas. Recently, submarine groundwater discharge was also proposed as a key source of substances (e.g., nutrients, carbon, metals, etc.) for the China seas (Liu et al., 2012; Wang et al., 2018; Wang et al., 2019). The China seas also have close hydrological and biogeochemical interactions with the North Pacific Ocean (Zheng et al., 2006; Song, 2010). Briefly speaking, river input, Kuroshio Current, and Asian Monsoon are the key external stressors inducing on the complicated ocean circulation and biogeochemical processes in the China seas.

2.2. ^{90}Sr analysis in seawater

In this study, we collected 40 L of surface seawater nearby the Fangchenggang Nuclear Power Plant (108.57°E, 21.68°N) in the Beibu Gulf, northwestern part of the South China Sea during 2016– 2018. The analytical method for ^{90}Sr in seawater was well validated by our passed proficiency test organized by the IAEA in 2016 (Deng et al., 2018). Additionally, the radiochemical procedure for ^{90}Sr in seawater has been described in previous studies (Yu et al., 2015; Deng et al., 2020).

In brief, seawater was immediately adjusted to pH = 1.0 with concentrated HNO_3 at the sampling date. The carriers of 200 mg Sr^{2+} and 40 mg Y^{3+} were added and mixed with seawater by stirring for 2 h in the land-based laboratory. A precipitate was formed after the addition of 30 g ammonium chloride (NH_4Cl) and 200 g sodium carbonate (Na_2CO_3). The precipitate was collected and dissolved with 6 M HNO_3 and adjusted to pH = 1. Afterwards, ^{90}Y and stable Y were extracted with 10% Bis-2-etylhexyl-phosphoric acid (HDEHP) in n-heptane. The ^{90}Y and stable Y were re-extracted into 6 M HNO_3 and precipitated at pH = 8– 9 with the concentrated $NH_3{\cdot}H_2O$. The precipitate was re-dissolved with concentrated HNO_3 and saturated oxalic acid was added at pH ~ 1. The precipitate of yttrium oxalate was weighed to calculate the chemical yield of Y and was measured with a gas-flow β counter (MPC9604, Ortec). The ^{90}Sr activity and its uncertainty in seawater were calculated using Eqs. (1)–(2).

$$A_0 = \frac{n_1 - n_0}{\varepsilon \eta V} \times \frac{\lambda_1 T}{1 - e^{-\lambda_1 T}} \times e^{\lambda_1 (t_2 - t_1)} \times e^{\lambda_0 (t_1 - t_0)} \quad (1)$$

$$\delta A_0 = A_0 \times \sqrt{\frac{n_1 + n_0}{T(n_1 - n_0)^2} + \left(\frac{\delta \varepsilon}{\varepsilon}\right)^2} \quad (2)$$

where A_0 and δA_0 are the ^{90}Sr activity and its associated uncertainty at the sampling date; n_1 and n_0 denote the β counting rate for the sample and the instrumental background, respectively; ε, η, and V refer to the detection efficiency, chemical yield of Y, and volume of seawater,

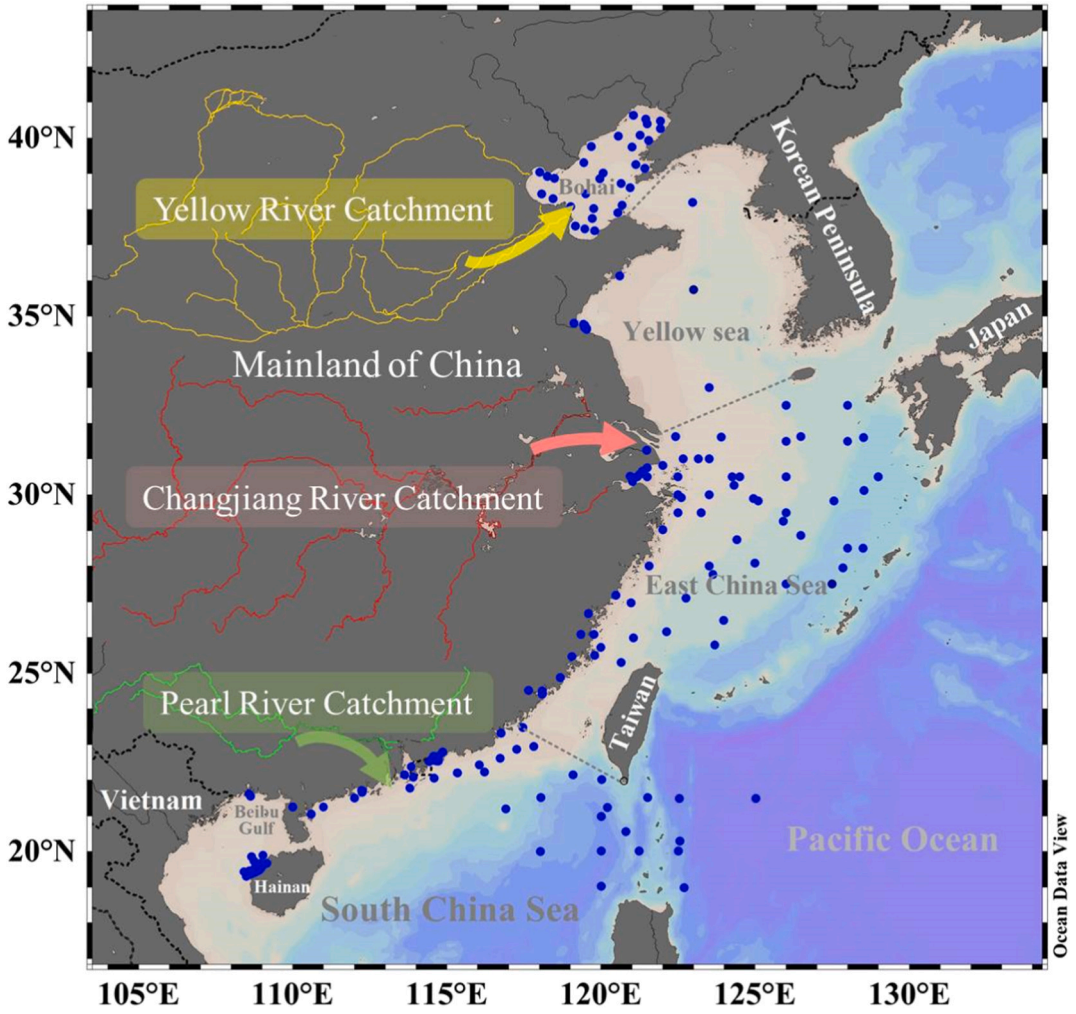

Fig. 1. Station map of ^{90}Sr in seawater of the China seas. The three largest rivers namely the Yellow River, Changjiang River, and Pearl River are also indicated.

respectively; t_0, t_1, t_2, and T are defined as the sampling date, separation date of ^{90}Y/^{90}Sr, detection date of ^{90}Y, and time interval for ^{90}Y measurement in the gas-flow β counter, respectively; λ_0 and λ_1 are decay constants of ^{90}Sr and ^{90}Y, respectively.

2.3. Data compilation

Large amounts of data on ^{90}Sr in seawater were compiled in the China seas, including the Bohai Sea during 1963– 2018 (Ministry of Ecology and Environment, n.d.; Li and Li, 1981; Zhao et al., 1988; Yao et al., 2010), Yellow Sea during 1963– 2016 (Li and Li, 1981; Liu et al., 1988; Jiang et al., 2005; Yao et al., 2010; Xu et al., 2011; Liu, 2018), East China Sea during 1963– 2016 (Ministry of Ecology and Environment, n.d.; Li and Li, 1981; Li et al., 1982; Zhao, 1988; Huo et al., 1994; Qian et al., 1998; Xu et al., 2013; Lin, 2017; Shao et al., 2018a), and South China Sea during 1984– 2018 (Liu, 1987; Liu et al., 1989; Wu et al., 1992; Chen, 1993; Chen et al., 1993; Lin and Zhou, 1995; Liu and Zhou, 2000; Chen et al., 2003; Ji and Zhang, 2004; Yao et al., 2010; Zhou et al., 2018; Zhu et al., 2018; Chen et al., 2019; Liu et al., 2020). All stations of the compiled data in the China seas are exhibited in Fig. 1. Note that many references were peer-reviewed and published in Chinese. The compilation of these ^{90}Sr data sets published in Chinese would facilitate international communication on historical ^{90}Sr activity in the China seas.

3. Results and discussion

3.1. Historical ^{90}Sr activity in the China seas

In addition to our ^{90}Sr data (0.84 Bq/m^3 ~ 1.07 Bq/m^3 in Fig. 2d) in the South China Sea during 2016–2018, we also compiled peer-reviewed and publicly available data on ^{90}Sr in seawater from the China seas. The historical ^{90}Sr data in the China seas are illustrated in Fig. 2. The ^{90}Sr activity was in the range of 0.73– 27.7 Bq/m^3 during 1963– 2018, 0.89– 10.2 Bq/m^3 during 1963– 2016, 1.3– 16.5 Bq/m^3 during 1963– 2016, and 0.84– 3.2 Bq/m^3 during 1984– 2018 in the Bohai Sea, Yellow Sea, East China Sea, and South China Sea, respectively. Additionally, an exponential function was fitted, as shown in Fig. 2. A decrease in ^{90}Sr activity (27.7 Bq/m^3, 10.2 Bq/m^3, and 7.30 Bq/m^3 in the Bohai Sea, Yellow Sea, and East China Sea in 1963) was observed from the high/middle latitude (Bohai Sea) to the low latitude (East China Sea), consistent with a decline in global fallout ^{90}Sr inventory from high/middle latitude to low latitude (Waters et al., 2015). The exponential decrease in ^{90}Sr activity in the China seas was also consistent with other studies on historical ^{90}Sr curves in seawater from the other marginal/coastal seas, such as the Baltic Sea (Saniewski and Zalewska, 2018), Italian coast (Cigna, 2006), East Sea/Sea of Japan (Hirose and Povinec, 2019), and Japanese coast (Cigna, 2006), and from the open oceans, such as the Pacific Ocean and Indian Ocean (Povinec et al., 2005). The ^{90}Sr activity in seawater from the China seas was about 1.0 Bq/m^3 in 2018 and was comparable to the ^{90}Sr baseline before the FNA (~1.0 Bq/

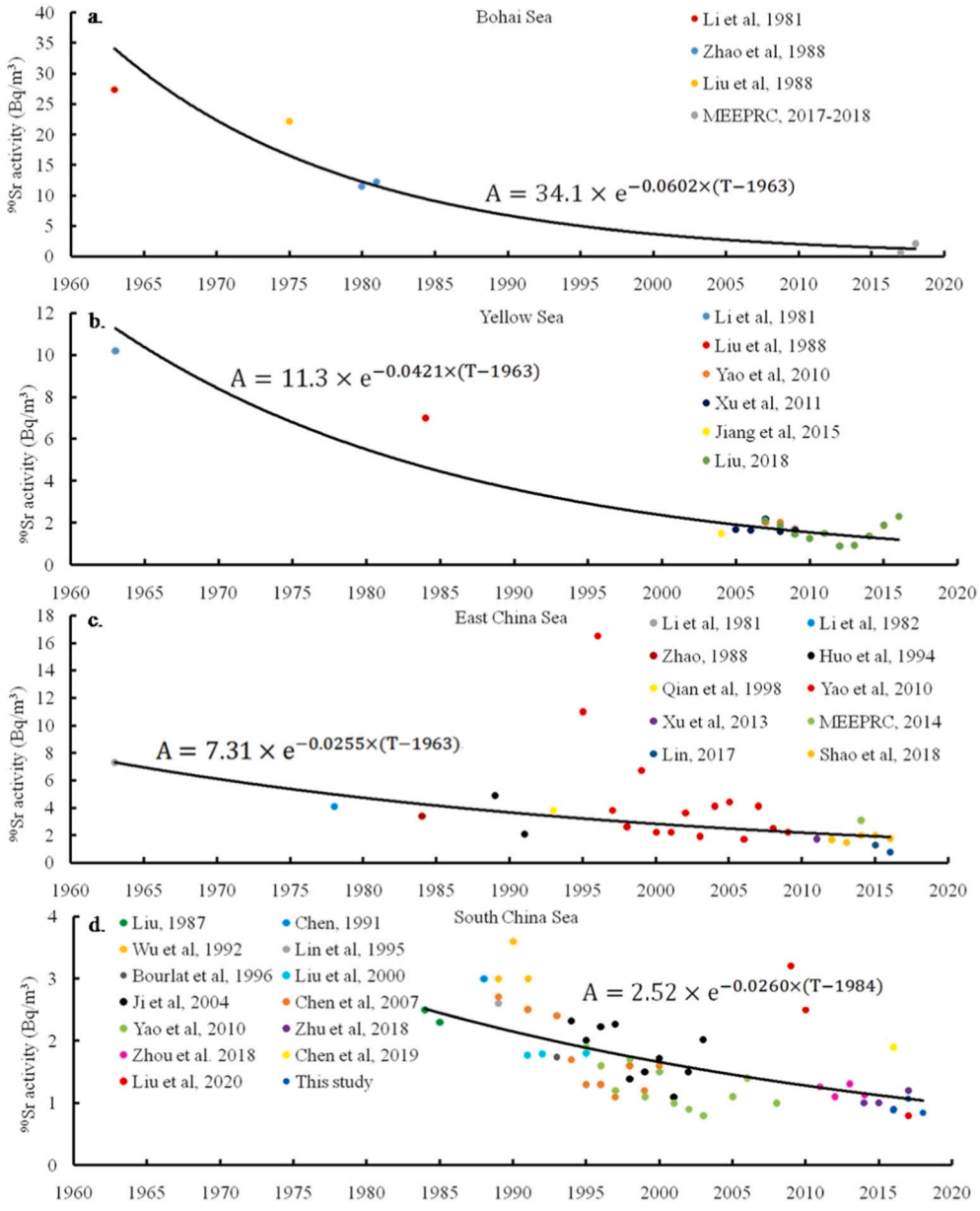

Fig. 2. Historical ^{90}Sr activity in seawater from the Bohai Sea (a), Yellow Sea (b), East China Sea (c), and South China Sea (d).

m^3) in the North Pacific Ocean (Povinec et al., 2005). Notice that the ^{90}Sr activity in seawater from the China seas in 2018 was significantly lower than that from the Baltic Sea (5.6– 8.7 Bq/m^3) during 1998– 2016 (Saniewski and Zalewska, 2018). We found that ^{90}Sr activity in the China seas also lie at the lower end of the global range of ^{90}Sr activity (0.1– 49 Bq/m^3) in surface seawater provided by IAEA report (IAEA, 2005). Overall, historical ^{90}Sr data in the China seas from 1963 to 2018 would provide a valuable supplement to the existing ^{90}Sr database in the global ocean.

3.2. *Effective half-life of ^{90}Sr in the China seas in comparison with ^{137}Cs*

Based on the exponential decrease in ^{90}Sr activity in seawater (Fig. 2), the EHL of ^{90}Sr was fitted and quantified to be 11.5 ± 1.6 a in the Bohai Sea during 1963– 2018, 16.5 ± 2.4 a in the Yellow Sea during 1963– 2016, 27.2 ± 6.2 a in the East China Sea during 1963– 2016, and 26.7 ± 4.3 a in the South China Sea during 1984– 2018, respectively, in Fig. 3. It should be noted that the uncertainty of the EHL of ^{90}Sr is higher in the East China Sea, probably due to a more hydrodynamic and complicated ocean circulation pattern relative to the Bohai Sea, Yellow Sea, and South China Sea.

In this study, we found that the EHL of ^{90}Sr in the high latitude seas (Bohai Sea and Yellow Sea) was shorter than that in the low latitude seas (East China Sea and South China Sea), in consistent with the EHL of ^{137}Cs (Fig. 3). Correspondingly, a shorter EHL of ^{90}Sr was also observed in the North Pacific Ocean (12 ± 1 a) relative to the Equatorial Pacific Ocean (21 ± 2 a) in previous study (Povinec et al., 2005). The pattern of longer EHL of ^{90}Sr in the low-latitude sea/ocean was mainly attributed to the transport of ^{90}Sr from the middle/high latitude sea with higher atmospheric deposition flux, higher ^{90}Sr activity in seawater, and greater inventory of ^{90}Sr in seawater column derived from nuclear weapons testing. The continuous ^{90}Sr input into the low latitude sea and ocean from high latitudes would delay the exponential decrease in ^{90}Sr activity in seawater and lead to a longer EHL in the low latitude sea and ocean.

We also found that the EHL of ^{90}Sr in the East China Sea (27.2 ± 6.2 a) and South China Sea (26.7 ± 4.3 a) was slightly longer than that in the Equatorial Pacific Ocean (21 ± 2 a) (Povinec et al., 2005). The East

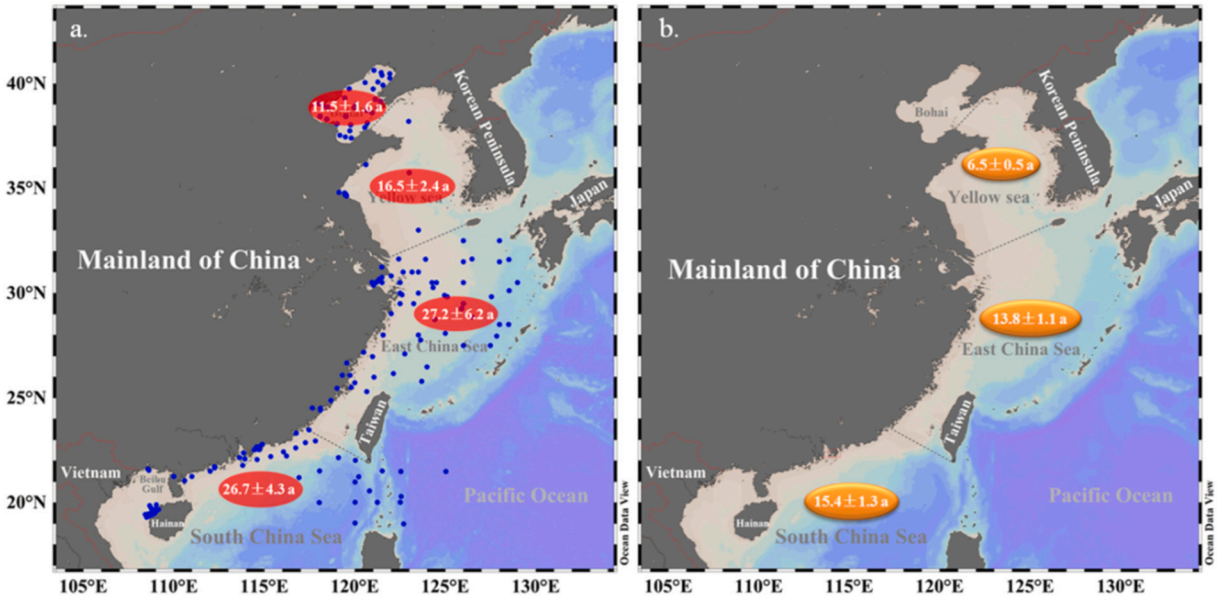

Fig. 3. Effective half-life (EHL) of ^{90}Sr (a) and ^{137}Cs (b) in seawater of the China seas. The EHL of ^{137}Cs was referenced to other study (Wu et al., 2020b).

China Sea and South China Sea have intensive exchange with the North Pacific Subtropical Gyre by the Kuroshio Current, which originates from the North Pacific Equatorial Current (Lie and Cho, 2016; Zhu et al., 2019). Additionally, large river input (e.g., the Changjiang River, the Pearl River) of ^{90}Sr would further delay the exponential decrease in ^{90}Sr activity in the marginal seas of East China Sea and South China Sea, leading to a longer EHL of ^{90}Sr relative to that in the Equatorial Pacific Ocean. Additionally, submarine groundwater discharge was also proposed as a potential source of ^{90}Sr to the East China Sea (Zhang et al., 2021). Therefore, the EHL of ^{90}Sr in the East China Sea (27.2 ± 6.2 a) and South China Sea (26.7 ± 4.3 a) was similar to but slightly longer than that in the Equatorial Pacific Ocean (21 ± 2 a).

The artificial radionuclide of ^{137}Cs with a physical half-life of 30.2 a exhibits conservative behavior in seawater. Hence, ^{137}Cs and ^{90}Sr are generally discussed together because of their similar physical half-lives and conservative behaviors in the ocean. The activity ratio of ^{90}Sr to ^{137}Cs is relatively stable with a value of ~0.63 in seawater (Povinec et al., 2012). The EHL of ^{137}Cs was calculated to be 6.5 ± 0.5 a, 13.8 ± 1.1 a, and 15.4 ± 1.3 a in the Yellow Sea, East China Sea, and South China Sea, respectively (Wu et al., 2020b). Overall, the EHL of ^{137}Cs was shorter than that of ^{90}Sr in the China seas (Fig. 3). A previous study also indicated a shorter EHL of ^{137}Cs (9.1 a) relative to EHL of ^{90}Sr (50.3 a) in the Baltic Sea, which was attributed to low mobility of ^{137}Cs relative to ^{90}Sr in the soil from the same catchment and followed by low flux of ^{137}Cs relative to ^{90}Sr by river discharging into the Baltic Sea (Saniewski and Zalewska, 2018). The activity of ^{137}Cs (0.74 ± 0.11 Bq/m^3) was significantly lower than that of ^{90}Sr in river water (10.4 ± 0.44 Bq/m^3) in Japan (Ikeuchi, 2003; Ikeuchi, 2006). The river flux of ^{90}Sr was also reported to be higher than that of ^{137}Cs into the Black Sea (Kanivets et al., 1999). Particularly, the ^{137}Cs activity was also observed to be lower than ^{90}Sr activity in the Changjiang River, Pearl River, and Yellow River (Ministry of Ecology and Environment, n.d.). Submarine groundwater discharge may also contribute to the surplus flux of ^{90}Sr relative to ^{137}Cs (Zhang et al., 2021). From the perspective of source for radionuclide, a higher flux of ^{90}Sr discharged into the China seas would delay the exponential decrease in ^{90}Sr activity in seawater, resulting in a long EHL of ^{90}Sr relative to that of ^{137}Cs.

Furthermore, ^{137}Cs is strongly associated with cation-exchange sites on particles (e.g., clay minerals) in seawater and passively scavenged into marine sediment (Zhang et al., 2019; Tachi et al., 2020). It was reported that ^{137}Cs could be efficiently scavenged in the marginal sea with a high concentration of suspended particles relative to the open ocean with a low concentration of suspended particles (Zhang et al., 2019; Yamada et al., 2021). The burial flux of ^{137}Cs in marine sediment was approximately three times higher than the ^{137}Cs fluxes of atmospheric deposition and river input in the Bohai Sea, Yellow Sea, and East China Sea (Zhang et al., 2019). A large amount of ^{137}Cs in seawater was transported from the open ocean (North Pacific Ocean) to coastal seas followed by sedimentation and burial in the marginal seas (Bohai Sea, Yellow Sea, and East China Sea) (Zhang et al., 2019). The phenomenon of boundary scavenging of ^{137}Cs in the marginal sea was also observed in the Arctic Ocean, which has a broad continental shelf (Kuzyk et al., 2013). Due to the high scavenging of ^{137}Cs in the marginal seas, the EHL of ^{137}Cs in the China seas (6.5– 15.4 a) was generally shorter than that in the open Pacific Ocean (13– 23 a) (Povinec et al., 2005; Wu, 2018; Zhang et al., 2019). The sediment-seawater distribution coefficient of ^{137}Cs (100–1000 L/kg) was calculated to be higher than that of ^{90}Sr (1–100 L/kg) in marine environments (IAEA, 2004; Takata et al., 2016). From the perspective of sink for radionuclide, high boundary scavenging of ^{137}Cs relative to ^{90}Sr may also result in a shorter EHL of ^{137}Cs relative to that of ^{90}Sr in the marginal seas.

3.3. *Contrasting patterns of EHL of ^{90}Sr and ^{137}Cs in the marginal seas and open oceans*

After compiling the available EHL of ^{90}Sr and ^{137}Cs in seawater from other seas and oceans, we found contrasting patterns of EHL of ^{90}Sr and ^{137}Cs in the marginal/coastal seas and open oceans (Fig. 4). Generally, the EHL of ^{90}Sr was longer than that of ^{137}Cs in all marginal seas of the Yellow Sea, East China Sea, South China Sea, East Sea/Sea of Japan (Hirose and Povinec, 2019), and Baltic Sea (Saniewski and Zalewska, 2018). By contrast, a slightly shorter EHL of ^{90}Sr relative to that of ^{137}Cs was observed in all open oceans of the North Pacific Ocean, South Pacific Ocean, and Equatorial Pacific Ocean (Povinec et al., 2005). These contrasting patterns of the ratio of EHL_{90Sr} to EHL_{137Cs} (EHL_{90Sr}/EHL_{137Cs}) in the marginal seas ($EHL_{90Sr}/EHL_{137Cs} > 1$ in Fig. 4) and open oceans ($EHL_{90Sr}/EHL_{137Cs} < 1$ in Fig. 4) are challenging the traditional understanding of similar behaviors between ^{90}Sr and ^{137}Cs in marine environments.

The EHL patterns of ^{90}Sr and ^{137}Cs in the marginal seas ($EHL_{90Sr}/EHL_{137Cs} > 1$) was closely related to the combined effects of the sources of high river input and submarine groundwater discharge of ^{90}Sr relative

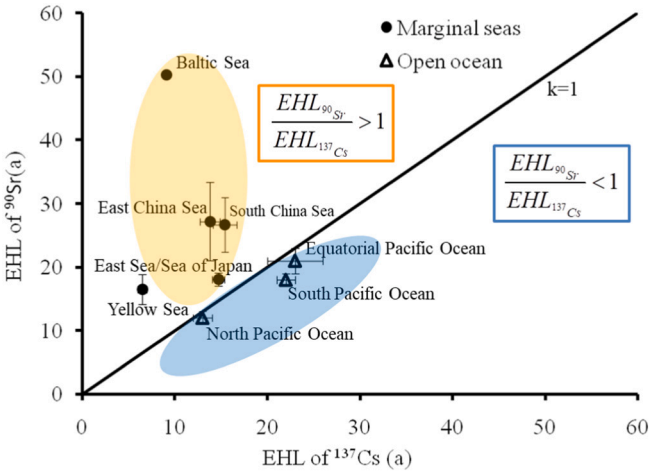

Fig. 4. Contrasting patterns of the EHL of ^{90}Sr and ^{137}Cs in the marginal seas and open oceans.

to ^{137}Cs (high value of S for ^{90}Sr in Eq. (3)) and the sink of intensive boundary scavenging of ^{137}Cs by passive adsorption onto the particle surface (high value of k for ^{137}Cs relative to that for ^{90}Srin Eq. (3)) (Ikeuchi, 2006; Kuzyk et al., 2013; Saniewski and Zalewska, 2018; Zhang et al., 2019). By contrast, the pattern of EHL of ^{90}Sr and ^{137}Cs in the open oceans ($EHL_{90Sr}/EHL_{137Cs} < 1$) may be attributed to the distinct sinking pathways of ^{90}Sr and ^{137}Cs by the marine biological pumps (hard tissue pump for ^{90}Sr and soft tissue pump for ^{137}Cs in Fig. 5) for actively scavenging artificial radionuclides. ^{90}Sr behaves like calcium and is preferentially incorporated into biominerals (e.g. $SrSO_4$ in radiolarian (de Villiers, 1999), $Sr_XCa_{(10-X)}(PO_4)_6(OH)_2$ in fish bone and otolith (Fujimoto et al., 2015; Koarai et al., 2020), $(Ca/Sr)CO_3$ in coral skeleton (Lin et al., 2019)) with relatively high density to be gravitationally settled out of the surface ocean, leading to a low residence time of ^{90}Sr (high value of k for ^{90}Sr in Eq. (3)) and a short EHL of ^{90}Sr in the surface seawater of open oceans. Correspondingly, ^{137}Cs is analogous to potassium and is preferentially stored in soft tissue (e.g., particulate organic material) with a relatively low density, resulting in high efficiency of ^{137}Cs recycling in the upper ocean and delaying the decline in ^{137}Cs activity (low value of k for ^{137}Cs in Eq. (3)) with long EHL of ^{137}Cs in the surface seawater of open oceans.

$$\frac{dA}{dt} = D\frac{\partial^2 A}{\partial x^2} - u\frac{\partial A}{\partial x} - \lambda A - kA + S \quad (3)$$

Additionally, we further checked the simultaneous measurements for the vertical profiles of ^{90}Sr and ^{137}Cs activity in the marginal sea of the East China Sea (Zhang et al., 2021) and the open Pacific Ocean (Hamilton, 2005). The activity ratio of ^{137}Cs/^{90}Sr in seawater increased with the depth at the stations CJ, D9, and G8 in the marginal sea of the East China Sea (Zhang et al., 2021), but the activity ratio of ^{137}Cs/^{90}Sr decreased with the depth near the Tuamoto Archipelago in the open Pacific Ocean (Hamilton, 2005). The contrasting patterns of the activity ratio of ^{137}Cs/^{90}Sr in seawater were probably attributed to the high efficiency of transferring ^{137}Cs into the ocean interior relative to ^{90}Sr by preferentially passive adsorption of ^{137}Cs onto the particle surface in the marginal sea (high intensity of boundary scavenging) and to high efficiency of ^{90}Sr export from the surface ocean by active hard tissue pump for ^{90}Sr scavenging relative to ^{137}Cs scavenging in the open ocean, leading to an increasing trend of ^{137}Cs/^{90}Sr with the depth in the marginal sea and decreasing trend of ^{137}Cs/^{90}Sr with the depth in the open ocean, respectively. Consequently, on the basis of the above-mentioned field observations and theoretical analysis, the subtly different processes of ^{90}Sr and ^{137}Cs in the marginal seas and open oceans are illustrated in Fig. 5.

The artificial radionuclides of ^{90}Sr and ^{137}Cs are typical cases of short-term perturbations and distinct responses in contemporary marine environments. The proxies of δ^7Li and ^{10}Be/^{9}Be, which belong to the same group as ^{137}Cs (alkali metal) and ^{90}Sr (alkaline-earth metal) in the periodic table of elements, were measured in marine environment to reconstruct continental weathering that controls the carbon cycle and climate over geological history (Willenbring and von Blanckenburg, 2010; Misra and Froelich, 2012). However, the discrepancy in continental weathering history based on distinct proxies of δ^7Li and ^{10}Be/^{9}Be was observed in the marginal seas and open oceans (Willenbring and von Blanckenburg, 2010; Misra and Froelich, 2012). The distinct responses of ^{90}Sr and ^{137}Cs in specific marine environments (marginal seas or open oceans) may provide insights into some perturbation events of weathering input of alkali metals (e.g., Li isotopes and K isotopes) and alkaline-earth metals (Be isotopes, Mg isotopes, and Sr isotopes) and subsequent records in ancient marine environments.

3.4. Possible signal of Fukushima-derived ^{90}Sr in the China seas

It was reported that a large amount of ^{90}Sr was released into marine environment by direct discharging of the cooling seawater after the FNA

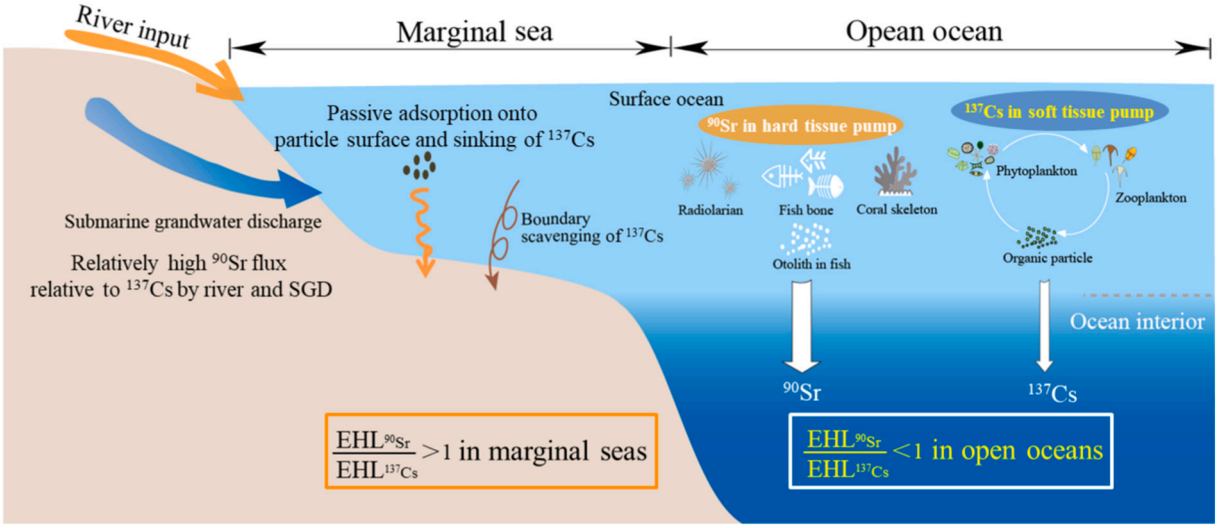

Fig. 5. Schematic diagram of distinct sources and sinks of ^{90}Sr and ^{137}Cs in the marginal seas and open oceans.

(Castrillejo et al., 2016). The maximum ^{90}Sr activity in seawater was reported to be 400,000 Bq/m^3 after the FNA relative to the value of ~1.0 Bq/m^3 before the FNA (Povinec et al., 2012). Several studies indicated that the ^{90}Sr activity in seawater surrounding Japan in 2016 declined to the baseline level (~1.0 Bq/m^3) before the FNA due to intensive hydrodynamic conditions off the Japanese East Coast (Guard, n.d.; Karube et al., 2016; IAEA, 2019). However, the polluted sea area gradually enlarged after the dispersion of Fukushima-derived ^{90}Sr in the North Pacific Ocean.

Theoretically, the China seas may have received Fukushima-derived radionuclides transported by ocean circulation (Zhao et al., 2021). Actually, few stations were observed with ^{134}Cs activity in seawater derived from the FNA above the minimum detection activity (MDA) in the Yellow Sea (0.1– 0.2 Bq/m^3) in July 2014 (Inoue et al., 2018a), the East China Sea (0.29 Bq/m^3) in November 2013 (Wang et al., 2022), and the South China Sea (0.2 Bq/m^3) during November to December 2012 (Deng et al., 2020), despite many stations with ^{134}Cs bellow MDA in the China seas (Men et al., 2015; Zhou et al., 2018; Wang et al., 2022). The measured ^{134}Cs derived from the FNA in the Yellow Sea and South China Sea was reported to be influenced by the Kuroshio Current with elevated ^{134}Cs activity (~0.5–1.0 Bq/m^3 during 2013– 2016) in seawater (Inoue et al., 2018b). ^{134}Cs should not occur before the FNA due to its short physical half-life (2.06 a). Therefore, the proxy of ^{134}Cs without any residual signal from global fallout was highly sensitive and widely used to identify the impact of the FNA.

The recent status of ^{90}Sr activity in seawater (in the period of 2016–2018) was about 1– 2 Bq/m^3 in the China seas (Fig. 2) and was also close to the ^{90}Sr baseline (~1.0 Bq/m^3) in the North Pacific Ocean before the FNA (Povinec et al., 2012). It was reported that ^{90}Sr derived from the FNA was not identified in the East China Sea and South China Sea during 2011– 2014 (Men et al., 2015; Zhou et al., 2018; Deng et al., 2020). The ^{90}Sr activity was variable in a relatively large range of <0.56– 2.62 Bq/m^3 in the South China Sea during 2011– 2014 (Zhou et al., 2018). Additionally, the source term of ^{90}Sr in seawater derived from the FNA was two to three orders of magnitude lower than that of ^{134}Cs and ^{137}Cs derived from the FNA (Lin et al., 2016). ^{90}Sr derived from the FNA in Kuroshio seawater was conservatively calculated to be 0.01 Bq/m^3 based on Fukushima-derived ^{134}Cs in Kuroshio seawater (~1.0 Bq/m^3) and Fukushima-derived ^{90}Sr/^{134}Cs activity ratio (0.01) (Lin et al., 2016; Inoue et al., 2018b). The Fukushima-derived ^{90}Sr activity in seawater from the China seas should be lower than 0.01 Bq/m^3 if we further consider the mixing ratio of distinct water masses from the Kuroshio Current and the China seas. Actually, the uncertainty of ^{90}Sr activity (~0.1 Bq/m^3) in seawater derived from the measurement by the gas-flow β counter is generally one order of magnitude higher than Fukushima-derived ^{90}Sr activity in seawater from the China seas (0.01 Bq/m^3). It should be difficult to identify ^{90}Sr derived from the FNA in the China seas after taking seasonal/annual variation of ^{90}Sr activity and its uncertainty derived from radiochemical measurement into account. Theoretical calculation is a necessary and beneficial supplement to the limited frequency of the field observation of ^{90}Sr in the China seas.

4. Conclusion

A long-term time series of ^{90}Sr activity in seawater was established in the China seas during 1963– 2018 after compiling our measured ^{90}Sr data together with many previous studies. The EHL of ^{90}Sr was calculated to be 11.5 ± 1.6 a, 16.5 ± 2.4 a, 27.2 ± 6.2 a, and 26.7 ± 4.3 a in the Bohai Sea, Yellow Sea, East China Sea, and South China Sea, respectively. The EHL of ^{90}Sr was longer than that of ^{137}Cs in the China seas due to the higher sources of river input and submarine groundwater discharge of ^{90}Sr and the sink of intensive boundary scavenging of ^{137}Cs. By contrast, the EHL of ^{90}Sr was shorter than that of ^{137}Cs in the open oceans probably because of higher efficiency of hard tissue pump for scavenging ^{90}Sr relative to soft tissue pump for scavenging ^{137}Cs. The contrasting patterns in the EHL of ^{90}Sr and ^{137}Cs revealed subtly different behaviors of ^{90}Sr and ^{137}Cs in contemporary marine environment. Finally, Fukushima-derived ^{90}Sr was not clearly identified on the basis of the limited frequency of the field observation of ^{90}Sr in the China seas. The lack of significant Fukushima-derived ^{90}Sr in the China seas was also explained by theoretical analysis after taking seasonal/annual variation of ^{90}Sr activity and its uncertainty derived from radiochemical measurement into account. It is recommended that ^{134}Cs would be a better proxy for tracking the signal from the FNA due to high sensitivity of ^{134}Cs with no residual from global fallout. However, the short half-life of ^{134}Cs (2.06 a) will also result in the decay of ^{134}Cs in seawater and challenge its feasibility for detecting the signal from the FNA in the future.

The historical ^{90}Sr activity in the China seas will provide a valuable supplement to the limited long-term time series of ^{90}Sr monitoring in the global ocean and consolidate the ability to identify artificial radionuclides from nuclear accidents, nuclear reprocessing plants, and radioactive waste dumping sites in the context of the rapid expansion of nuclear power plants construction in Asia. Our work would also provide the key parameter of the EHL in marine models for predicting the ^{90}Sr activity in the China seas and enhance our understanding of ^{90}Sr behavior and its fate in marine environments. Additionally, the distinct pathways of ^{90}Sr and ^{137}Cs in the contemporary marine environment may provide insights into the different behaviors of δ^7Li and ^{10}Be/^{9}Be in the ancient marine environment, especially for the distinct responses between the marginal seas and open oceans.

CRediT authorship contribution statement

Wuhui Lin: Conceptualization, Investigation, Methodology, Writing – original draft, Funding acquisition. **Minting Mo:** Methodology, Visualization. **Kefu Yu:** Conceptualization, Investigation, Resources, Writing – original draft. **Jinqiu Du:** Conceptualization, Methodology. **Hongtao Shen:** Conceptualization, Funding acquisition. **Yinghui Wang:** Conceptualization, Investigation, Methodology. **Xianwen He:** Investigation, Methodology, Resources. **Liangliang Feng:** Investigation, Methodology.

Declaration of competing interest

The authors declare that they have no known competing financial interests or personal relationships that could have appeared to influence the work reported in this paper.

Acknowledgements

This study was financially supported by the National Natural Science Foundation of China (41906043, 42030502, and 42090041), the Natural Science Foundation of Guangxi Province (2021GXNSFAA220053 and 2019GXNSFAA185006), and the Open Project of Guangxi Key Laboratory of Nuclear Physics and Nuclear Technology (NLK2021-04).

References

Buesseler, K.O., 2020. Opening the floodgates at Fukushima. Science 369 (6504), 621–622. https://doi.org/10.1126/science.abc1507.

Buesseler, K., Dai, M., Aoyama, M., Benitez nelson, C., Charmasson, S., Higley, K., Maderich, V., Masqué, P., Oughton, D., Smith, J.N., 2017. Fukushima Daiichi-derived radionuclides in the ocean: transport, fate, and impacts. Annu. Rev. Mar. Sci. 9 (1), 173–203. https://doi.org/10.1146/annurev-marine-010816-060733.

Burger, A., Lichtscheidl, I., 2019. Strontium in the environment: review about reactions of plants towards stable and radioactive strontium isotopes. Sci. Total Environ. 653, 1458–1512. https://doi.org/10.1016/j.scitotenv.2018.10.312.

Cao, L., Zheng, J., Zhou, Z., Bu, W., Wang, Z., Zheng, W., Yamada, M., 2021. Distribution and behavior of plutonium isotopes in Western Pacific marginal seas. Catena 198, 105023. https://doi.org/10.1016/j.catena.2020.105023.

Casacuberta, N., Masqué, P., Garcia-Orellana, J., Garcia-Tenorio, R., Buesseler, K., 2013. 90Sr and 89Sr in seawater off Japan as a consequence of the Fukushima Dai-ichi nuclear accident. Biogeosciences 10, 3649–3659. https://doi.org/10.5194/bg-10-3649-2013.

Castrillejo, M., Casacuberta, N., Breier, C.F., Pike, S.M., Masque, P., Buesseler, K.O., 2016. Reassessment of 90Sr, 137Cs and 134Cs in the coast off Japan derived from the Fukushima Dai-ichi nuclear accident. Environ. Sci. Technol. 50 (1), 173–180. https://doi.org/10.1021/acs.est.5b03903.

Chen, J., 1993. Distribution of U,90Sr,137Cs,3H and gross Beta radioactivity in offshore water of South China Sea. Mar. Sci. 17 (1), 69–70 (in Chinese).

Chen, J., Wu, S., Shi, C., Xu, P.A., Zeng, X., 1993. Comprehensive study of radioactive background in the coastal waters of South China Sea area. J. Isot. 6 (1), 41–46 (in Chinese).

Chen, Z., Lin, Q., Deng, F., Liu, Y., Song, H., Li, L., 2003. Radioactivity levels of nuclides 90Sr and 137Cs in marine media around Daya Bay nuclear power plant. In: Compilation of Papers from National Symposium on Radioactive Effluent and Environmental Monitoring and Evaluation (in Chinese).

Chen, B., Peng, C., Zhou, H., He, X., Lu, Y., 2019. Investigation of 90Sr radioactivity level in the environment of Fangchenggang nuclear power plant during initial operation period. Chin.J.Radiol.Health (in Chinese) 28 (5), 575–578. https://doi.org/10.13491/j.issn.1004-714x.2019.05.027 (in Chinese).

Cigna, A.A., 2006. Forty years of anthropogenic radionuclides in surface seawater.Italian and Japanese data. Ocean Sci. J. 41 (4), 261–290. https://doi.org/10.1007/BF03020630.

Corcho-Alvarado, J.A., Balsiger, B., Sahli, H., Astner, M., Byrde, F., Röllin, S., Holzer, R., Mosimann, N., Wüthrich, S., Jakob, A., Burger, M., 2016. Long-term behavior of 90Sr and 137Cs in the environment: case studies in Switzerland. J. Environ. Radioact. 160, 54–63. https://doi.org/10.1016/j.jenvrad.2016.04.027.

de Villiers, S., 1999. Seawater strontium and Sr/Ca variability in the Atlantic and Pacific oceans. Earth Planet. Sci. Lett. 171 (4), 623–634. https://doi.org/10.1016/S0012-821X(99)00174-0.

Deng, F., Lin, W., Lin, J., Yu, W., Li, Y., Yu, T., 2018. International comparison of 90Sr analysis in seawater. Mar. Environ. Sci. 37 (3), 448–451. https://doi.org/10.13634/j.cnki.mes.2018.03.021 (In Chinese).

Deng, F., Lin, F., Yu, W., He, J., Wang, F., Chen, Z., 2020. The distributions of 134Cs, 137Cs and 90Sr in the northwest Pacific seawater in the winter of 2012. Mar. Pollut. Bull. 152, 110900 https://doi.org/10.1016/j.marpolbul.2020.110900.

Eyrolle, F., Lepage, H., Antonelli, C., Morereau, A., Cossonnet, C., Boyer, P., Gurriaran, R., 2020. Radionuclides in waters and suspended sediments in the Rhone River (France) - current contents, anthropic pressures and trajectories. Sci. Total Environ. 723, 137873 https://doi.org/10.1016/j.scitotenv.2020.137873.

Fujimoto, K., Miki, S., Kaeriyama, H., Shigenobu, Y., Takagi, K., Ambe, D., Ono, T., Watanabe, T., Morinaga, K., Nakata, K., 2015. Use of otolith for detecting strontium-90 in fish from the harbor of Fukushima Dai-ichi Nuclear Power Plant. Environ. Sci. Technol. 49 (12), 7294–7301. https://doi.org/10.1021/es5051315.

Guard, J.C.. Annual Reports of Radioactivity Survey for 1999–2018 (in Japanese). from. https://www1.kaiho.mlit.go.jp/KANKYO/OSEN/housha.html.

Hamilton, T.F., 2005. Linking legacies of the Cold War to arrival of anthropogenic radionuclides in the oceans through the 20th century. In: Radioactivity in the Environment, 6. Elsevier, Livingston, H. D., pp. 23–78

Hirose, K., Povinec, P.P., 2019. 137Cs and 90Sr in surface waters of the Sea of Japan: variations and the Fukushima Dai-ichi Nuclear Power Plant accident impact. Mar. Pollut. Bull. 146, 645–652. https://doi.org/10.1016/j.marpolbul.2019.07.024.

Huo, X., Chen, Y., Yao, J., Yang, J., 1994. Radioactivity level in the coastal waters of the East China Sea. Mar. Environ. Sci. 13 (2), 23–27 (in Chinese).

IAEA, 2004. Sediment Distribution Coefficients And Concentration Factors for Biota in the Marine Environment. IAEA, Vienna.

IAEA, 2005. Worldwide Marine Radioactivity Studies (WOMARS): Radionuclide Levels in Oceans And Seas. IAEA, Vienna.

IAEA, 2019. Interlaboratory Comparisons 2014–2016: Determination of Radionuclides in Sea Water, Sediment And Fish.

Igarashi, Y., Kajino, M., Zaizen, Y., Adachi, K., Mikami, M., 2015. Atmospheric radioactivity over Tsukuba, Japan: a summary of three years of observations after the FDNPP accident. Prog.EarthPlanet.Sci. 2 (1), 1–19. https://doi.org/10.1186/s40645-015-0066-1.

Ikeuchi, Y., 2003. Temporal variations of 90Sr and 137Cs concentrations in Japanese coastal surface seawater and sediments from 1974 to 1998. Deep-Sea Res. II Top. Stud. Oceanogr. 50 (17), 2713–2726. https://doi.org/10.1016/S0967-0645(03)00143-7.

Ikeuchi, Y., 2006. Temporal variations and behaviour of 90Sr and 137Cs in precipitation, river water and seawater in Japan. In: Povinec, P.P., Sanchez-Cabeza, J.A. (Eds.), Radioactivity in the Environment, 8. Elsevier, pp. 397–405. https://doi.org/10.1016/S1569-4860(05)08032-0.

Inoue, M., Shirotani, Y., Nagao, S., Aramaki, T., Kim, Y.I., Hayakawa, K., 2018a. Spatial variations of 226Ra, 228Ra, 134Cs, and 137Cs concentrations in western and southern waters off the Korean Peninsula in July 2014. J. Environ. Radioact. 182, 151–156. https://doi.org/10.1016/j.jenvrad.2017.11.020.

Inoue, M., Shirotani, Y., Yamashita, S., Takata, H., Kofuji, H., Ambe, D., Honda, N., Yagi, Y., Nagao, S., 2018b. Temporal and spatial variations of 134Cs and 137Cs levels in the Sea of Japan and Pacific coastal region: implications for dispersion of FDNPP-derived radiocesium. J. Environ. Radioact. 182, 142–150. https://doi.org/10.1016/j.jenvrad.2017.11.032.

Ji, C., Zhang, D., 2004. Results and analysis of environmental radiation monitoring at GNPS (1994–2003). Radiat. Prot. 24 (3–4), 173–188. https://doi.org/10.1007/BF02911033 (in Chinese).

Jiang, K., Tian, Q., Gou, Q., Chen, Z., 2005. TNPS environmental monitoring in 2004 (pre-operation). Radiat. Prot. 25 (6), 321–331 (in Chinese).

Johansen, M.P., Ruedig, E., Tagami, K., Uchida, S., Higley, K., Beresford, N., 2015. Radiological dose rates to marine fish from the Fukushima Daiichi accident: the first three years across the North Pacific. Environ. Sci. Technol. 49 (3), 1277–1285. https://doi.org/10.1021/es505064d.

Kanivets, V.V., Voitsekhovitch, O.V., Simov, V.G., Golubeva, Z.A., 1999. The post-Chernobyl budget of 137Cs and 90Sr in the Black Sea. J. Environ. Radioact. 43 (2), 121–135. https://doi.org/10.1016/S0265-931X(98)00087-3.

Karube, Z.I., Inuzuka, Y., Tanaka, A., Kurishima, K., Kihou, N., Shibata, Y., 2016. Radiostrontium monitoring of bivalves from the Pacific coast of eastern Japan. Environ. Sci. Pollut. Res. 23 (17), 17095–17104. https://doi.org/10.1007/s11356-016-6878-8.

Kasamatsu, F., Inatomi, N., 1998. Effective environmental half-lives of 90Sr and 137Cs in the coastal seawater of Japan. J. GeophysRes. Oceans 103 (C1), 1209–1217. https://doi.org/10.1029/97JC02807.

Kenyon, J.A., Buesseler, K.O., Casacuberta, N., Castrillejo, M., Otosaka, S., Masqué, P., Drysdale, J.A., Pike, S.M., Sanial, V., 2020. Distribution and evolution of Fukushima Dai-ichi derived 137Cs, 90Sr, and 129I in surface seawater off the coast of Japan. Environ. Sci. Technol. 54 (23), 15066–15075. https://doi.org/10.1021/acs.est.0c05321.

Kinase, T., Adachi, K., Sekiyama, T.T., Kajino, M., Zaizen, Y., Igarashi, Y., 2020. Temporal variations of 90Sr and 137Cs in atmospheric depositions after the Fukushima Daiichi Nuclear Power Plant accident with long-term observations. Sci. Rep. 10 (1), 21627. https://doi.org/10.1038/s41598-020-78312-3.

Koarai, K., Kino, Y., Oka, T., Takahashi, A., Suzuki, T., Shimizu, Y., Chiba, M., Osaka, K., Sasaki, K., Urushihara, Y., Fukuda, T., Isogai, E., Yamashiro, H., Fukumoto, M., Sekine, T., Shinoda, H., 2020. Incorporation and accumulation of strontium-90 in the hard tissue of animals and their relationship with strontium-90 pollution in the environment. In: Fukumoto, M. (Ed.), Low-dose Radiation Effects on Animals And Ecosystems: Long-term Study on the Fukushima Nuclear Accident. Springer Singapore, Singapore, pp. 53–62.

Kuzyk, Z.Z.A., Gobeil, C., Macdonald, R.W., 2013. 210Pb and 137Cs in margin sediments of the Arctic Ocean: controls on boundary scavenging. Glob. Biogeochem. Cycles 27 (2), 422–439. https://doi.org/10.1002/gbc.20041.

Li, P., Li, J., 1981. The determination of 90Sr and gross Beta in surface seawater in Chinese coasts. Oceanol. Limnol. Sin. 12 (4), 332–340.

Li, P., Yu, Y., Yuan, Y., 1982. The contents of strontium-90 in surface seawater in East China Sea and its adjacent region. Trans. Oceanol. Limnol. 4 (3), 18–22 (in Chinese).

Lie, H.-J., Cho, C.-H., 2016. Seasonal circulation patterns of the yellow and East China seas derived from satellite-tracked drifter trajectories and hydrographic observations. Prog. Oceanogr. 146, 121–141. https://doi.org/10.1016/j.pocean.2016.06.004.

Lin, Y., 2017. Analysis of the radioactivity level of 90Sr in the coastal waters of Fujian province and the seawater surrounding the nuclear power plant. Chem.Eng.Equip.(in Chinese) 42 (8), 288–289. https://doi.org/10.19566/j.cnki.cn35-1285/tq.2017.08.115 (in Chinese).

Lin, B., Zhou, Z., 1995. Investigation of 90Sr activity level of Daya Bay coastal areas in Guangdong. Radiat. Prot. 15 (2), 129–137 (in Chinese).

Lin, W., Chen, L., Yu, W., Ma, H., Zeng, Z., Lin, J., Zeng, S., 2015. Radioactivity impacts of the Fukushima Nuclear Accident on the atmosphere. Atmos. Environ. 102, 311–322. https://doi.org/10.1016/j.atmosenv.2014.11.047.

Lin, W., Chen, L., Yu, W., Ma, H., Zeng, Z., Zeng, S., 2016. Radioactive source terms of the Fukushima Nuclear Accident. Sci. China: Earth Sci. 59 (1), 214–222. https://doi.org/10.1007/s11430-015-5112-8.

Lin, W., Yu, K., Deng, F., Wang, Y., Feng, Y., Liu, X., Mo, Z., Ma, H., 2019. Fingerprints of radionuclides in modern coral skeletons in the South China Sea. China Environ. Sci. 39 (10), 4279–4289. https://doi.org/10.19674/j.cnki.issn1000-6923.2019.0499 (In Chinese).

Lin, W., Yu, K., Du, J., Lin, H., Yu, W., Mo, M., 2021. Consequences of marine ecological environment and our preparedness for Fukushima radioactive wastewater discharge into the ocean. Chin. Sci. Bull. 66 (35), 4500–4509. https://doi.org/10.1360/TB-2021-0743.

Liu, H., 1987. The content and distribution of artificical radionuclide 90Sr in the offshore water in South China Sea. Mar. Sci. 11 (5), 36–37 (in Chinese).

Liu, J., 2018. Results and analysis of peripheral radiation environmental monitoring of Tianwan nuclear power station. Pollut. Control Technol. 31 (2), 65–70 (in Chinese).

Liu, G., Zhou, C., 2000. Contents and behavior characteristics of 137Cs and 90Sr in various mediums of Daya Bay. J.Oceanogr.TaiWan Strait (in Chinese) 19 (3), 261–268 (in Chinese).

Liu, X., Chen, M., Zhao, D., Zhang, Z., Sun, P., 1988. The status of radioactivity in the offshore of Qingdao. J. Oceanogr. Huanghai Bohai Seas 6 (2), 30–38 (in Chinese).

Liu, H., Chen, Z., Liang, Q., 1989. Study of distribution character of artificial radioactives 90Sr, 137Cs in the Zhujiang estuary area in South China Sea. Mar. Sci. 13 (1), 62–64 (in Chinese).

Liu, Q., Dai, M., Chen, W., Huh, C.-A., Wang, G., Li, Q., Charette, M.A., 2012. How significant is submarine groundwater discharge and its associated dissolved inorganic carbon in a river-dominated shelf system? Biogeosciences 9, 1777–1795. https://doi.org/10.5194/bg-9-1777-2012.

Liu, W., Qi, Y., Lin, F., Zhang, W., Wang, X., 2020. Result analysis of two marine radioactivity surveys in the adjacent waters of Hainan Changjiang NPP. J. Appl. Oceanogr. 39 (1), 63–70. https://doi.org/10.3969/J.ISSN.2095-4972.2020.01.009 (in Chinese).

Men, W., He, J., Wang, F., Wen, Y., Li, Y., Huang, J., Y, X., 2015. Radioactive status of seawater in the northwest Pacific more than one year after the Fukushima nuclear accident. Sci. Rep. 5, 7757 https://doi.org/10.1038/srep07757.

Men, W., Deng, F., He, J., Yu, W., Wang, F., Li, Y., Lin, F., Lin, J., Lin, L., Zhang, Y., 2017. Radioactive impacts on nekton species in the Northwest Pacific and humans more than one year after the Fukushima nuclear accident. Ecotoxicol. Environ. Saf. 144, 601–610. https://doi.org/10.1016/j.ecoenv.2017.06.042.

Merz, S., Shozugawa, K., Steinhauser, G., 2016. Effective and ecological half-lives of 90Sr and 137Cs observed in wheat and rice in Japan. J. Radioanal. Nucl. Chem. 307 (3), 1807–1810. https://doi.org/10.1007/s10967-015-4352-6.

Miki, S., Fujimoto, K., Shigenobu, Y., Ambe, D., Kaeriyama, H., Takagi, K., Ono, T., Watanabe, T., Sugisaki, H., Morita, T., 2017. Concentrations of 90Sr and 137Cs/90Sr activity ratios in marine fishes after the Fukushima Dai-ichi Nuclear Power Plant accident. Fish. Oceanogr. 26 (2), 221–233. https://doi.org/10.1111/fog.12182.

Ministry of Ecology and Environment. National Environmental Radiation Quality Report of China during 2014-2018 (in Chinese). from. http://www.mee.gov.cn/hjzl/hjzlqt/hyfshj/.

Misra, S., Froelich, P.N., 2012. Lithium isotope history of Cenozoic seawater: changes in silicate weathering and reverse weathering. Science 335 (6070), 818–823. https://doi.org/10.1126/science.1214697.

Morita, T., Fujimoto, K., Kasai, H., Yamada, H., Nishiuchi, K., 2010. Temporal variations of 90Sr and 137Cs concentrations and the 137Cs/90Sr activity ratio in marine brown algae, Undaria pinnatifida and Laminaria longissima, collected in coastal areas of Japan. J. Environ. Monit. 12 (5), 1179–1186. https://doi.org/10.1039/B920173D.

Nagaoka, M., Yokoyama, H., Fujita, H., Nakano, M., Watanabe, H., Sumiya, S., 2015. Spatial distribution of radionuclides in seabed sediments off Ibaraki coast after the Fukushima Daiichi Nuclear Power Plant accident. J. Radioanal. Nucl. Chem. 303 (2), 1305–1308. https://doi.org/10.1007/s10967-014-3633-9.

Pan, K., Wang, W.-X., 2012. Trace metal contamination in estuarine and coastal environments in China. Sci. Total Environ. 421–422, 3–16. https://doi.org/10.1016/j.scitotenv.2011.03.013.

Pan, K., Tan, Q.-G., Wang, W.-X., 2016. Two-compartment kinetic modeling of radiocesium accumulation in marine bivalves under hypothetical exposure regimes. Environ. Sci. Technol. 50 (5), 2677–2684. https://doi.org/10.1021/acs.est.5b05445.

Povinec, P.P., Aarkrog, A., Buesseler, K.O., Delfanti, R., Hirose, K., Hong, G.H., Ito, T., Livingston, H.D., Nies, H., Noshkin, V.E., 2005. 90Sr, 137Cs and 239,240Pu concentration surface water time series in the Pacific and Indian Oceans–WOMARS results. J. Environ. Radioact. 81 (1), 63–87. https://doi.org/10.1016/j.jenvrad.2004.12.003.

Povinec, P.P., Hirose, K., Aoyama, M., 2012. Radiostrontium in the western North Pacific: characteristics, behavior, and the Fukushima impact. Environ. Sci. Technol. 46 (18), 10356–10363. https://doi.org/10.1021/es301997c.

Pröhl, G., Ehlken, S., Fiedler, I., Kirchner, G., Klemt, E., Zibold, G., 2006. Ecological half-lives of 90Sr and 137Cs in terrestrial and aquatic ecosystems. J. Environ. Radioact. 91 (1), 41–72. https://doi.org/10.1016/j.jenvrad.2006.08.004.

Qian, L., Cai, F., Lin, Q., Chen, Y., 1998. Behavior and characteristics of 90Sr in Xiamen estuarine and harbor area. Mar. Environ. Sci. 17 (2), 24–28 (in Chinese).

Robison, W.L., Conrado, C.L., Bogen, K.T., Stoker, A.C., 2003. The effective and environmental half-life of 137Cs at Coral Islands at the former US nuclear test site. J. Environ. Radioact. 69 (3), 207–223. https://doi.org/10.1016/S0265-931X(03)00080-8.

Saniewski, M., Zalewska, T., 2016. Atmospheric deposition and riverine load of 90Sr and 137Cs to the Gulf of Gdańsk (southern Baltic Sea) in the period 2005–2011. J. Environ. Radioact. 151, 1–11. https://doi.org/10.1016/j.jenvrad.2015.09.010.

Saniewski, M., Zalewska, T., 2018. Budget of 90Sr in the Gulf of Gdańsk (southern Baltic Sea). Oceanologia 60 (3), 256–263. https://doi.org/10.1016/j.oceano.2017.11.002.

Shao, L., Chen, Q., Zhou, Y., Lu, Y., Huang, W., Zhen, C., 2018a. Monitoring and analysis of the radiation level of Zhejiang province caused by Sr-90 in Fujian Ningde nuclear power station. Energy Environ. Prot. 32 (6), 50–52 (in Chinese).

Shao, Y., Yang, G., Tazoe, H., Ma, L., Yamada, M., Xu, D., 2018b. A review of measurement methodologies and their applications to environmental 90Sr. J. Environ. Radioact. 192, 321–333. https://doi.org/10.1016/j.jenvrad.2018.07.013.

Shozugawa, K., Riebe, B., Walther, C., Brandl, A., Steinhauser, G., 2015. Fukushima-derived radionuclides in sediments of the Japanese Pacific Ocean coast and various Japanese water samples (seawater, tap water, and coolant water of Fukushima Daiichi reactor unit 5). J. Radioanal. Nucl. Chem. 1–7 https://doi.org/10.1007/s10967-015-4386-9.

Song, J., 2010. Biogeochemical Processes of Biogenic Elements in China Marginal Seas. Springer, Berlin.

Steinhauser, G., 2014. Fukushima's forgotten radionuclides: a review of the understudied radioactive emissions. Environ. Sci. Technol. 48, 4649–4663. https://doi.org/10.1021/es405654c.

Tachi, Y., Sato, T., Takeda, C., Ishidera, T., Fujiwara, K., Iijima, K., 2020. Key factors controlling radiocesium sorption and fixation in river sediments around the Fukushima Daiichi Nuclear Power Plant. Part 2: sorption and fixation behaviors and their relationship to sediment properties. Sci. Total Environ. 724, 138097 https://doi.org/10.1016/j.scitotenv.2020.138097.

Takata, H., Tagami, K., Aono, T., Uchida, S., 2014. Distribution coefficients (Kd) of strontium and significance of oxides and organic matter in controlling its partitioning in coastal regions of Japan. Sci. Total Environ. 490, 979–986. https://doi.org/10.1016/j.scitotenv.2014.05.101.

Takata, H., Aono, T., Tagami, K., Uchida, S., 2016. A new approach to evaluate factors controlling elemental sediment–seawater distribution coefficients (Kd) in coastal regions,Japan. Sci. Total Environ. 543, 315–325. https://doi.org/10.1016/j.scitotenv.2015.11.034.

TEPCO, 2021. Radiation concentrations measured at the multi-nuclide removal equipment (ALPS) outlet (as of March 31, 2021). Retrieved 9 June, 2021, from. http://www.tepco.co.jp/en/decommission/progress/watertreatment/images/exit_en.pdf.

Vajda, N., Kim, C.-K., 2010. Determination of radiostrontium isotopes: a review of analytical methodology. Appl. Radiat. Isot. 68 (12), 2306–2326. https://doi.org/10.1016/j.apradiso.2010.05.013.

Wang, X., Baskaran, M., Su, K., Du, J., 2018. The important role of submarine groundwater discharge (SGD) to derive nutrient fluxes into River dominated Ocean Margins – the East China Sea. Mar. Chem. 204, 121–132. https://doi.org/10.1016/j.marchem.2018.05.010.

Wang, Q., Li, H., Zhang, Y., Wang, X., Zhang, C., Xiao, K., Qu, W., 2019. Evaluations of submarine groundwater discharge and associated heavy metal fluxes in Bohai Bay, China. Sci. Total Environ. 695, 133873 https://doi.org/10.1016/j.scitotenv.2019.133873.

Wang, F., Men, W., Yu, T., Huang, J., He, J., Lin, J., Lin, F., Deng, F., 2022. Intrusion of Fukushima-derived radiocesium into the East China Sea and the Northeast South China Sea in 2011–2015. Chemosphere 133546. https://doi.org/10.1016/j.chemosphere.2022.133546.

Waters, C.N., Syvitski, J.P.M., Gałuszka, A., Hancock, G.J., Zalasiewicz, J., Cearreta, A., Grinevald, J., Jeandel, C., Mcneill, J.R., Summerhayes, C., 2015. Can nuclear weapons fallout mark the beginning of the Anthropocene Epoch? Bull. At. Sci. 71 (3), 46–57. https://doi.org/10.1177/0096340215581357.

Willenbring, J.K., von Blanckenburg, F., 2010. Long-term stability of global erosion rates and weathering during late-Cenozoic cooling. Nature 465 (7295), 211–214. https://doi.org/10.1038/nature09044.

Wu, J., 2018. Impacts of Fukushima Daiichi Nuclear Power Plant accident on the Western North Pacific and the China Seas: evaluation based on field observation of 137Cs. Mar. Pollut. Bull. 127, 45–53. https://doi.org/10.1016/j.marpolbul.2017.11.056.

Wu, S., Shi, C., Chen, J., 1992. Distribution of 90Sr and 137Cs in coastal surface waters of Guangdong. J.Oceanogr.TaiWan Strait (in Chinese) 11 (4), 363–367 (in Chinese).

Wu, J., Sun, J., Xiao, X., 2020a. An overview of current knowledge concerning the inventory and sources of plutonium in the China Seas. Mar. Pollut. Bull. 150, 110599 https://doi.org/10.1016/j.marpolbul.2019.110599.

Wu, J., Xiao, X., Sun, J., 2020b. Distribution and budget of 137Cs in the China Seas. Sci. Rep. 10 (1), 8795. https://doi.org/10.1038/s41598-020-65280-x.

Xu, P., Jiang, Y., Wang, L., 2011. Radioactivity level of strontium-90 in peripheral water after operation of Tianwan nuclear power plant. Chin. J. Radiol. Health 20 (3), 334–335 (in Chinese).

Xu, C., Li, Z.E., Cheng, X., Xu, R., 2013. Assessment of radioactivity in seawater adjacent to Qinshan nuclear power plant. Environ. Chem. 32 (3), 518–519. https://doi.org/10.7524/j.issn.0254-6108.2013.03.027 (in Chinese).

Yamada, M., Oikawa, S., Shirotani, Y., Kusakabe, M., Shindo, K., 2021. Transuranic nuclides Pu, Am and Cm isotopes, and 90Sr in seafloor sediments off the Fukushima Daiichi Nuclear Power Plant during the period from 2012 to 2019. J. Environ. Radioact. 227, 106459 https://doi.org/10.1016/j.jenvrad.2020.106459.

Yao, H., Zhu, L., Zhou, Y., Shen, F., Liang, M., Cao, Z., Ye, J., 2010. Monitoring of radioactivity levels of sea water in near coast marine environment in China during 1995–2009. Radiat. Prot. Bull. 30 (5), 13–17 (in Chinese).

Yu, W., He, J., Lin, W., Li, Y., Men, W., Wang, F., Huang, J., 2015. Distribution and risk assessment of radionuclides released by Fukushima nuclear accident at the northwest Pacific. J. Environ. Radioact. 142, 54–61. https://doi.org/10.1016/j.jenvrad.2015.01.005.

Zhang, F., Wang, J., Liu, D., Bi, Q., Du, J., 2019. Distribution of 137Cs in the Bohai Sea, Yellow Sea and East China Sea: sources, budgets and environmental implications. Sci. Total Environ. 672, 1004–1016. https://doi.org/10.1016/j.scitotenv.2019.04.001.

Zhang, F., Wang, J., Bi, Q., Du, J., 2021. 90Sr in seawater of the East China Sea: inventory, new potential source, and environmental implications. Sci. Total Environ. 764, 144266 https://doi.org/10.1016/j.scitotenv.2020.144266.

Zhao, D., 1988. Radioactive 90Sr in Kuroshio Basin of East China Sea. Mar. Environ. Sci. 7 (3), 23–26 (in Chinese).

Zhao, D., Chen, M., Xi, Y., 1988. The study of the distribution of 90Sr in marine environment of Bohai Sea. Mar. Sci. 12 (2), 34–39 (in Chinese).

Zhao, C., Wang, G., Zhang, M., Wang, G., de With, G., Bezhenar, R., Maderich, V., Xia, C., Zhao, B., Jung, K.T., Periáñez, R., Akhir, M.F., Sangmanee, C., Qiao, F., 2021. Transport and dispersion of tritium from the radioactive water of the Fukushima Daiichi Nuclear Plant. Mar. Pollut. Bull. 169, 112515 https://doi.org/10.1016/j.marpolbul.2021.112515.

Zheng, Q., Fang, G., Song, Y.T., 2006. Introduction to special section: dynamics and circulation of the Yellow, East, and South China Seas. J. GeophysRes. Oceans 111, C11S01. https://doi.org/10.1029/2005JC003261.

Zhou, P., Li, D., Zhao, L., Li, H., Zhao, F., Zheng, Y., Fang, H., Lou, Q., Cai, W., 2018. Radioactive status of seawater and its assessment in the northeast South China Sea and the Luzon Strait and its adjacent areas from 2011 to 2014. Mar. Pollut. Bull. 131, 163–173. https://doi.org/10.1016/j.marpolbul.2018.04.009.

Zhu, S., Chen, R., Zhang, J., 2018. Investigation on Sr-90 radioactivity level in seawater of external environment of Yangjiang nuclear power plant. Resour.Econ.Environ. Prot.(in Chinese) 14 (8), 84–85. https://doi.org/10.16317/j.cnki.12-1377/x.2018.08.065 (in Chinese).

Zhu, Y., Sun, J., Wang, Y., Li, S., Xu, T., Wei, Z., Qu, T., 2019. Overview of the multi-layer circulation in the South China Sea. Prog. Oceanogr. 175, 171–182. https://doi.org/10.1016/j.pocean.2019.04.001.